Simultaneous 3D location and size measurement of bubbles and irregular sand particles using interferometric out-of-focus imaging

Lila Ouldarbi[1], Huanhuan Shen[1], Gaële Perret[2], Sébastien Coëtmellec[1], Gérard Gréhan[1], Denis Lebrun[1], Marc Brunel[1,*]

[1] UMR 6614 CORIA, Normandie Université, CNRS, Université et INSA de Rouen, Saint-Etienne du Rouvray, France
[2] UMR 6294 LOMC, Normandie Université, CNRS, Université du Havre, Le Havre, France
*corresponding author: marc.brunel@coria.fr

Abstract We present the realization of set-up where a cylindrical lens is used to determine the 3D positions of bubbles in a flow: the transverse position of a bubble is deduced from the transverse position of its interferometric out-of-focus image on the CCD sensor, its size is deduced from the fringe's frequency, and its longitudinal position from the orientation of the fringes. The effect introduced by the cylindrical lens (rotation of the fringes versus the longitudinal position of the bubble) can be induced by the pipe itself when the liquid and the bubbles are in a cylindrical pipe. When irregular particles as sand particles are present in the flow, the classical ways of interpretation do not work. The out-of-focus image of a sand particle is indeed a speckle-like pattern. We present a new original set-up which gives simultaneously the 3D location and the size of bubbles, and the 3D location and the size of sand particles as well. Air bubbles and grains of sand in a water-filled aquarium are illuminated by a Nd:YAG laser. The light scattered by the particles is collected at 45° by an optical system, which consists of a spherical lens, a diaphragm and a cylindrical lens aligned with a CCD camera. To corroborate the validity of the set-up, we compare simulated out-of-focus images with experimental acquisitions. Such a device should be a useful tool to study how water current turbines alter the seabed.
Keywords: Bubbles, Light scattering, Irregular particles, interferometric particle imaging

1 Introduction

Three-dimensional (3D) characterization of multiphasic flows has important applications. Different techniques have been proposed in the last decade. 3D PIV is particularly attractive, but requires many CCD sensors [1]. A complex signal processing is necessary to ensure the tomographic reconstruction of the flow. Plenoptic cameras offer an alternative with a single exposure [2]. Unfortunately, resolution is not so good. Digital holography uses only one standard camera [3]. The reconstruction and analysis of holograms can be time-consuming. Defocusing methods give an alternative way: they have allowed the 3D imaging of fluorescently doped tracers using a single camera [4]. For droplet or bubble characterization, interferometric out-of-focus imaging gives the possibility to determine their 2D positions in a laser sheet, their sizes and velocities using double-pulse acquisition [5-10]. In addition, high speed image processing techniques can be developed [11]. Unfortunately, the analysis over three spatial coordinate directions (i.e. in a volume) remains difficult. We have proposed recently some cylindrical set-ups which allow a characterization of droplets or bubbles in a volume [12-14]. We present here these recent developments, and show finally that the technique can be applied to the characterization of both bubbles and irregular particles in a volume. Bubbles are characterized using a classical fringe's analysis. Irregular sand grains are analyzed from the interpretation of their speckle-like out-of-focus image [15-17].

2 Principle of cylindrical interferometric out-of-focus imaging for the analysis of bubbles in a volume

Figure 1 shows the typical set-up of an interferometric laser imager for droplet sizing. Droplets are illuminated by a laser sheet [5]. Some part of the light is reflected by the droplet and one part is refracted by the droplet (without any internal reflection) [18-20]. The droplet is then observed in an out-of-focus plane with a lens or an objective. The defocused image is a circular spot with parallel interference fringes due to the two previous optical paths. It allows to determine the position of the droplets in the plane of the laser sheet and their sizes.

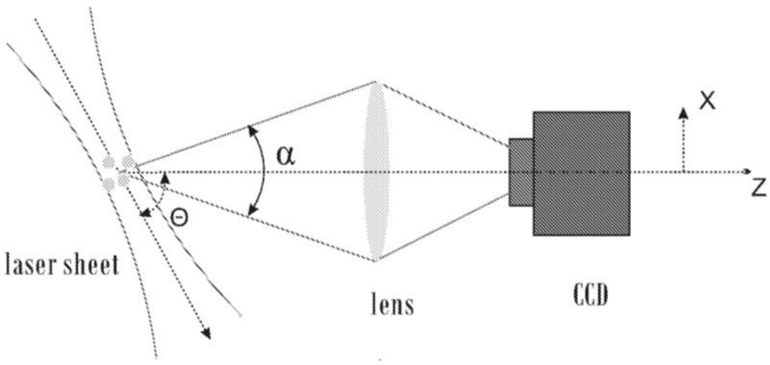

Fig. 1 Typical ILIDS set-up

In order to extend the technique to the analysis of droplets in a 3D volume, droplets have to be illuminated by a large plane wave beam. The longitudinal position z of each droplet (see figure 1) is then deduced from the diameter of the out-of-focus image. Another solution we proposed recently is to record images of droplets using a cylindrical imaging system. The longitudinal position of the droplets is given by the ellipticity of the out-of-focus image and /or by the orientation of the interference fringes [12,13]. Similar set-up can be used when investigating bubbles in a liquid [14].

Figure 2 shows the first set-up that has been realized. Bubbles are illuminated by a large collimated laser beam. The incidence angle of the laser on the aquarium is such that we observe light scattered at the scattering angle Θ=45°. At this angle, the amplitude of light reflected on the bubble and light refracted within the bubble are similar. The contrast of the interference fringes is then optimal. Interference occur as if light was emitted by two coherent sources: the glare points G_A and G_B of figure 3. In some cases, a third optical path can lead to the consideration of a third glare point: G_C, which will not be the case in these first experiments (the amplitude linked to this order remains small). The imaging system is composed of the association of a spherical lens and a cylindrical lens (CL). The main axes of the CL and of the CCD sensor are tilted with respect with the horizontal axis (see side view of figure 2). This orientation will cause the variation of the fringe orientation versus the longitudinal position of the bubbles.

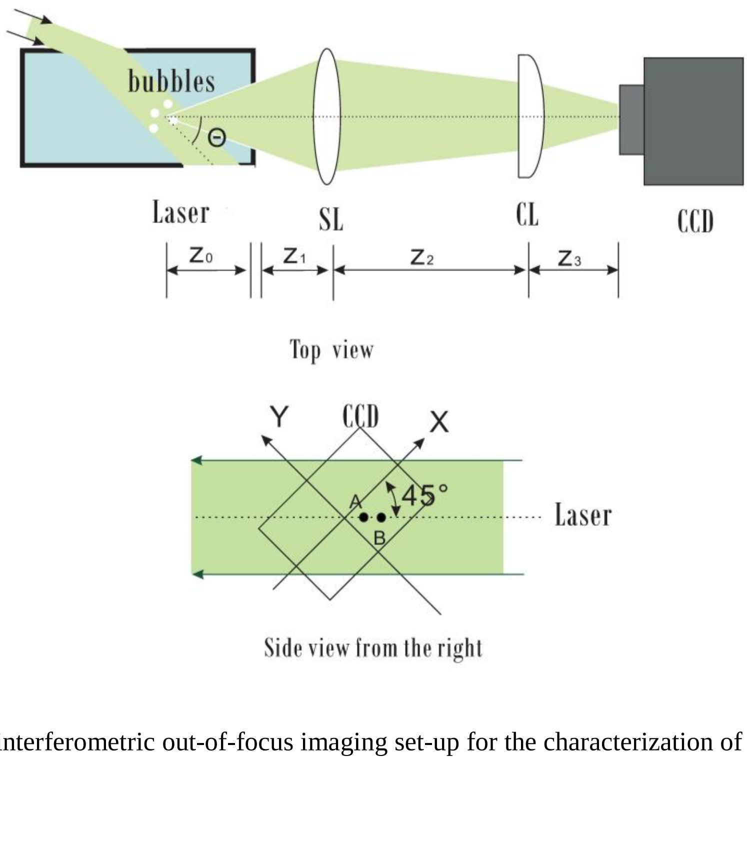

Fig. 2 Cylindrical interferometric out-of-focus imaging set-up for the characterization of bubbles in a volume

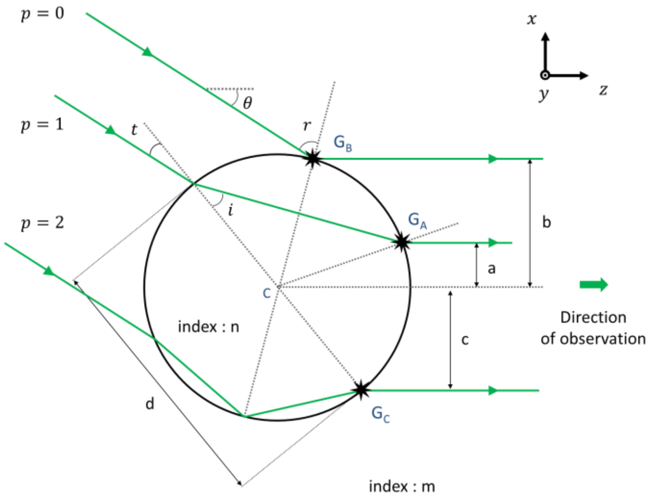

Fig. 3 Glare points of a bubble illuminated by a laser beam

This set-up can be modeled assuming that each scattering bubble can be described by two punctual emitters, i.e. the glare points G_A and G_B, and using a formalism based on generalized Huygens-Fresnel integrals [10,14]. The whole system is then described by its optical transfer matrix. The cylindrical geometry is described as well using different matrices along both transverse axes x and y. This model allows to calculate the longitudinal position of the particle versus the orientation of the fringes. This curve depends on the characteristics of the SL and CL, and on the different distances between the elements. In the case of the set-up we realized, it is plotted on figure 4. Parameters of the set-up are: z_1 = 108 mm; f_{SL} =100 mm; z_2 = 314 mm; $f_{CL;x}$ = 250 mm; $f_{CL;y}$ = +1; z_3 = 127 mm. The laser used is a frequency-doubled Nd:YAG laser emitting 4ns, 5 mJ pulses at the wavelength 532 nm.

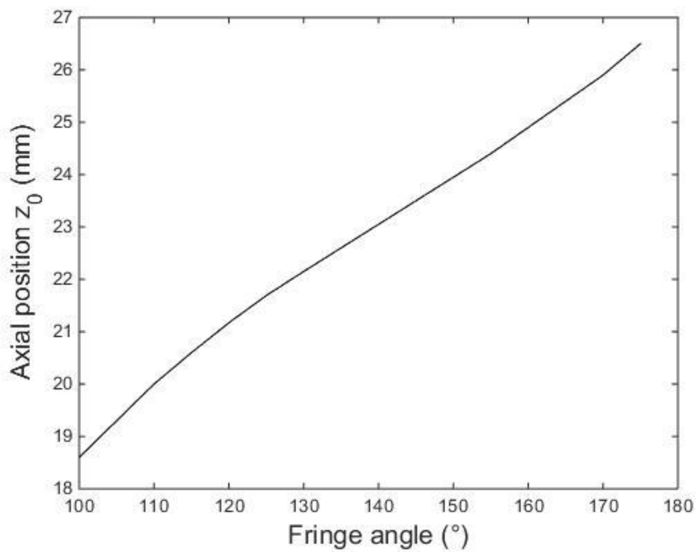

Fig. 4 Axial position of bubbles versus orientation of the fringes

Once the axial position of the bubbles is determined, analytical relations link the size of the bubble to the frequency of the fringes [14]. Figure 5 (on the left) shows a zoom of the experimental out-of-focus image of three droplets. We obtain respectively the following fringe angles from the left-hand sided to the right-hand sided bubble: $129 \pm 6°$, $131 \pm 8°$ 1, $101 \pm 3°$ .We deduce: $z_{0,\mathrm{bubble1}} = 22.1 \pm 0.7\mathrm{mm}$, $z_{0,\mathrm{bubble2}} = 22.3 \pm 0.8\mathrm{mm}$, $z_{0,\mathrm{bubble3}} = 18.8 \pm 0.4\mathrm{mm}$. We evaluate finally the diameter of a bubble from the frequency of the fringes. We obtain: $d_{\mathrm{bubble1}} = 185 \pm 20\mu\mathrm{m}$, $d_{\mathrm{bubble2}} = 153 \pm 20\mu\mathrm{m}$, $d_{\mathrm{bubble3}} =$

$200 \pm 12\mu m$. Finally, a simulation is done using these parameters. It is presented in figure 5 (on the right). It matches perfectly well the experimental image. This final fitting operation allows to reduce the uncertainty to $\pm 0.4mm$ for z_0, and to $\pm 8\mu m$ for d. We can note that the ellipticity of the out-of-focus image appears as another criterium to evaluate the axial position of the bubbles.

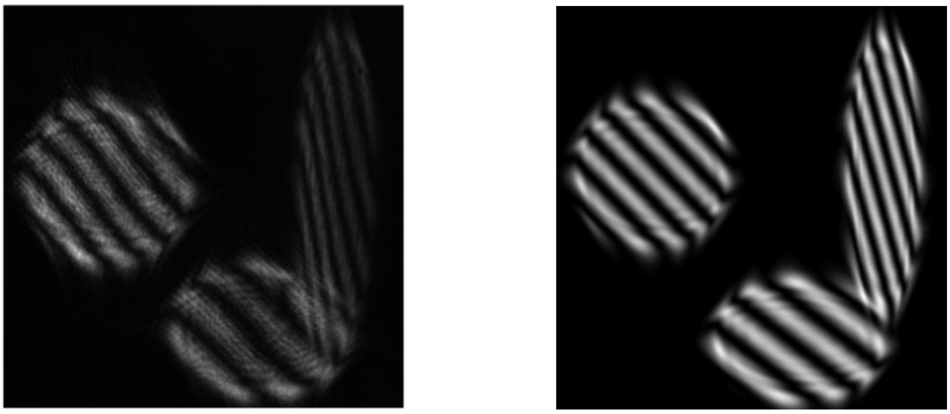

Fig. 5 Experimental (left) and corresponding simulated (right) out-of-focus images of three bubbles

3 Bubbles in a cylindrical channel

Figure 6 shows the second set-up that has been realized. Bubbles are illuminated by a large collimated laser beam. But bubbles are located in a cylindrical channel filled with water [21]. The incidence angle of the laser on the channel is such that we observe light scattered in an horizontal direction, at the scattering angle $\Theta=45°$.

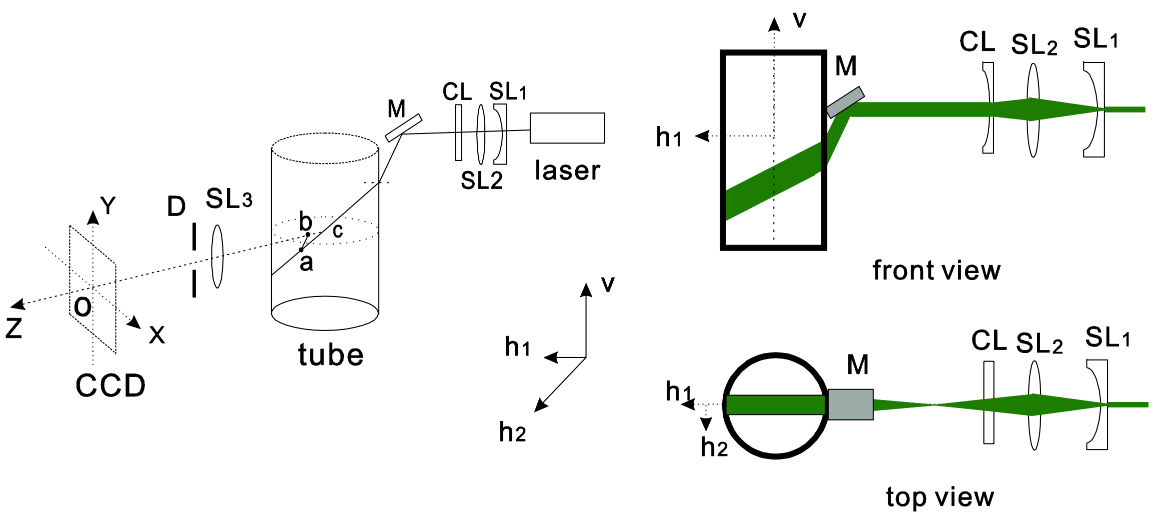

Fig. 6 Set-up for the characterization of bubbles in the volume of a cylindrical channel

Figure 7 (left) shows the out-of-focus image of two bubbles in the channel. Analyzing the angle of the fringes and their frequency, it is possible to evaluate the position of the bubbles and their sizes. The 3D positions of the two bubbles are (from the left-hand sided to the right-hand sided):

$$\vec{\mathbf{r}}_{\mathrm{bubble1}} = (0.027\mathrm{mm}, 0.226\mathrm{mm}, 149.4\mathrm{mm})$$
$$\vec{\mathbf{r}}_{\mathrm{bubble2}} = (0.143\mathrm{mm}, 0.712\mathrm{mm}, 147.6\mathrm{mm})$$

The radii of the two bubbles are : $\mathrm{R_{bubble1}} = 56.8\mu\mathrm{m}$, $\mathrm{R_{bubble2}} = 63.8\mu\mathrm{m}$. To validate these values, a complete simulation of the set-up using these parameters is done. It is presented in figure 7 (right). It matches very well the experimental results for the two bubbles that have been selected.

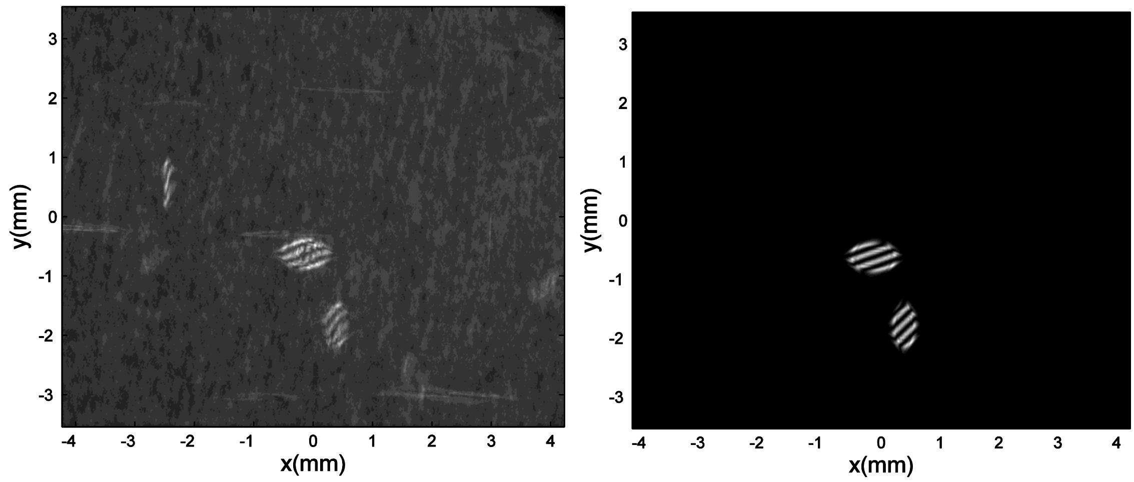

Fig. 7 Experimental (left) and corresponding simulated (right) out-of-focus images of two bubbles in a cylindrical channel.

4 Characterization of mixed sand particles and air bubbles in a volume

Let us now consider the most complex case when particles present in the fluid are either bubbles, or sand particles. The experimental set-up is presented in figure 8. Air bubbles and grains of sand in a water-filled aquarium are illuminated by a frequency-doubled Nd:YAG laser (4ns, 532 nm pulses). Light scattered by the particles is collected at 45° by an optical system. This imaging system is composed of a spherical lens (SL) and a cylindrical lens (CL). But in this case, the principal axes of the CL and of the CCD sensor are not rotated around the longitudinal z-axis. It means that the longitudinal position of the bubbles or particles will not be deduced from the orientation of the fringes but from the ellipticity of the out-of-focus images, as was previously mentioned. This is because there is no privileged orientation of fringes in the case of irregular sand particles. In this case, the interferometric image is indeed a speckle-like pattern. The distance between the particles and the wall of the aquarium is z_1 : it is an unknown parameter. The wall of aquarium is made of PMMA (thickness z_e = 10.2 mm, refractive index 1.495). Other distances are: z_2 = 122 mm, z_3 = 60.0 mm, z_4 = 64.0 mm, z_5 = 121 mm. Focus length of SL is 100 mm. Focus length of CL is 200 mm along the x-axis (infinity along y-axis). The dimensions of the CCD sensor are 2452x2054 pixels, for a pixel size of 3.45 µm.

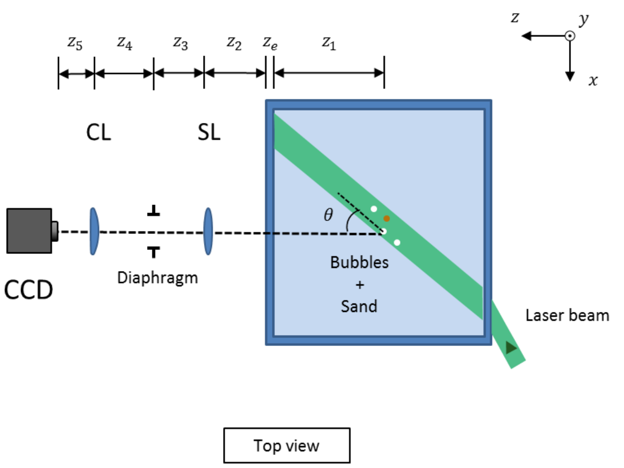

Fig. 8 Experimental set-up mixing sand and bubbles

Figure 9 shows the calibration curve giving the longitudinal position of the particle (bubble or irregular particle) versus the ellipticity of its out-of-focus image (ratio of the dimension along y- by dimension along x-axis). Figure 10 (left) shows a zoom on three particles of an out-of-focus image recorded with the CCD sensor. We see immediately that two objects are bubbles while the third one is an irregular grain of sand. With this set-up, the bubbles are characterized by low-frequency fringes with a high frequency modulation. This is due to the fact that three glare points have to be taken into account for this size of bubbles : the three glare points are the points G_A, G_B and G_C on figure 3.

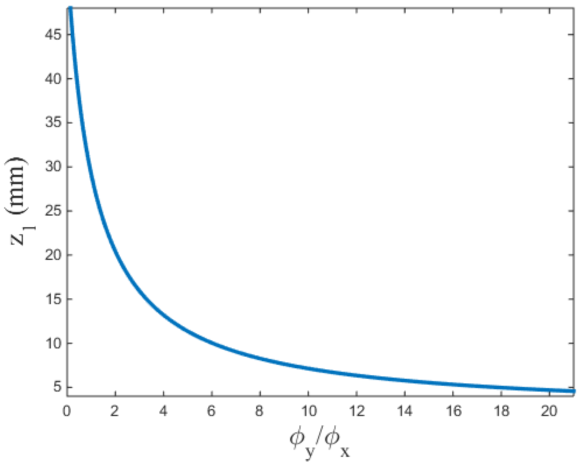

Fig. 9 longitudinal position of a particle (bubble or irregular particle) versus the ellipticity of its out-of-focus image

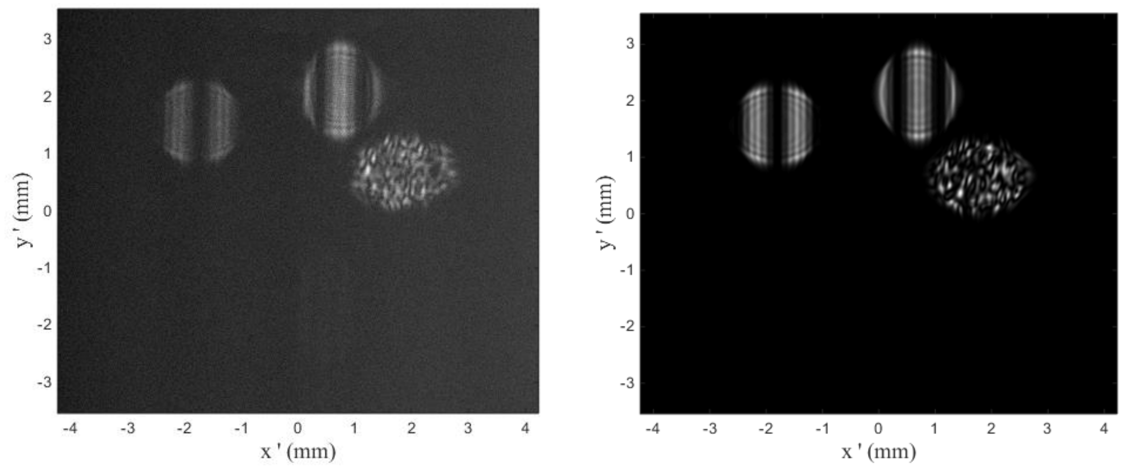

Fig. 10 Experimental out-of-focus image (left) and corresponding simulation (right)

From the ellipticity of each out-of-focus image, we deduce the longitudinal position of the particles according to figure 9. The transverse position of each bubble is deduced from the position of each elliptic image on CCD sensor. The diameter of the bubbles is deduced from the low fringe-frequency. The results obtained are presented in table 1.

Particle	x_0 (mm)	y_0 (mm)	z_0 (mm)	d (µm)
Bubble 1	1.439	-1.021	30.4	158.2
Bubble 2	-0.625	-1.363	26.4	137.5
Sand	1.463	-0.422	32.3	191.2 95.6

Table. 1 Position and size of the bubbles and sand particle

For the characterization of the sand particle, the procedure is more complex and is deduced from previous work [15,16]. The size of the speck of light in the speckle pattern is obtained statistically from the size of the central peak of the 2D-autocorrelation of the speckle pattern [22]. According to recent work done with irregular rough particles, the size of the speck of light along x-axis is inversely proportional to the size of the particle along axis x (idem along y-axis). Taking then into account the cylindrical geometry by the appropriate evaluation of the optical transfer matrix coefficients of the imaging system, we obtain the size of the sand particle. In our case, the particle has an elliptical shape. The dimension of the particle along its big-axis and along its small-axis are summarized in table 1. Figure 10 (right) shows a simulated out-of-focus image simulated using the parameters of table 1. For both bubbles, the agreement is very good. For the sand particle, it is not possible to reproduce a speckle pattern similar to the experimental one (there is no exact model that describes the scattering properties of an arbitrarily-shaped rough particle). The comparison that validates the procedure for this particle is the statistical size of the speck of light. This dimension is the same experimentally and numerically (the central peak of the 2D-autocorrelation for both experimental and simulated speckle patterns are not reported here but they have similar size and shape). The agreement is thus good as well. This is corroborated by the fact that sand particles in our experiment are ellipsoidal particles and have a calibrated size of 200 ± 30 µm along their biggest dimension.

5 Conclusion

We have presented the realization of set-up where a cylindrical lens is used to determine the 3D positions of bubbles in a flow: the transverse position of a bubble is deduced from the transverse position of its interferometric out-of-focus image on the CCD sensor, its size is deduced from the fringe's frequency, and its longitudinal position from the orientation of the fringes. The effect introduced by the cylindrical lens (rotation of the fringes versus the longitudinal position of the bubble) can be induced by the pipe itself when the liquid and the bubbles are in a cylindrical pipe. When irregular particles as sand particles are present in the flow, we show that their out-of-focus image is a speckle-like pattern, whose characteristics give the 3D position and the size of the rough particle. We present a new original set-up which gives simultaneously the 3D location and the size of bubbles, and the 3D location and the size of sand particles as well. To corroborate the validity of the set-up, we compare simulated out-of-focus images with experimental acquisitions. Such a device should be a useful tool to study how water current turbines alter the seabed.

Acknowledgments

The authors thank the French National Agency through the program Investissements d'Avenir (ANR-10-LABX-09-01) LabEx EMC^3

References

[1] Lindken R, Westerweel J, Wieneke B (2006) Stereoscopic micro particle image velocimetry, *Experiments in Fluids*, vol. 41, pp 161-171.

[2] Ng R, Levoy M, Bredif M, Duval G, Horowitz M, Hanrahan (2005) Light field photography with a handheld plenoptic camera,' Stanford University Computer Science Tech Report CSTR 2005-02 (2005).

[3] Pu Y, Meng H (2000) An advanced off-axis holographic particle image velocimetry (HPIV) system, *Experiments in Fluids*, vol. 29, pp 184-197.

[4] Lin D, Angarita-Jaimes N C, Chen S, Greenaway A H, Towers C E, Towers D P (2008) Three-dimensional particle imaging by defocusing method with an annular aperture, *Optics Letters*, vol. 33, pp 905-907. doi: http://dx.doi.org/10.1364/OL.33.000905

[5] Glover A R, Skippon S M, Boyle R D (1995) Interferometric laser imaging for droplet sizing: a method for droplet-size measurement in sparse spray systems. *Applied Optics*, vol. 34, pp 8409–8421. doi: http://dx.doi.org/10.1364/AO.34.008409

[6] Kawaguchi T, Akasaka Y, Maeda M (2002) Size measurements of droplets and bubbles by advanced interferometric laser imaging technique, *Measurement Science and Technology*, vol. 13, pp 308-316. doi: 10.1088/0957-0233/13/3/312

[7] Damaschke N, Nobach H, Tropea C (2002) Optical limits of particle concentration for multi-dimensional particle sizing techniques in fluid mechanics, *Experiments in Fluids*, vol. 32, pp 143-152. doi: 10.1007/s00348-001-0371-x

[8] Hardalupas Y., Sahu S., Taylor A.M.K.P., Zarogoulidis K (2010) Simultaneous planar measurement of droplet velocity and size with gas phase velocities in a spray by combined ILIDS and PIV techniques, *Experiments in Fluids*, vol. 49, pp 417-434. doi: 10.1007/s00348-009-0802-7

[9] Lacagnina G, Grizzi S, Falchi M, Di Felice F, Romano G P (2011) Simultaneous size and velocity measurements of cavitating microbubbles using interferometric laser imaging, *Experiments in Fluids*, vol. 50, pp 1153-1167. doi: 10.1007/s00348-011-1055-9

[10] Shen H, Coetmellec S, Grehan G, Brunel M (2012) ILIDS revisited: elaboration of transfer matrix models for the description of complete systems, *Applied Optics*, vol. 51, pp 5357-5368. doi: http://dx.doi.org/10.1364/AO.51.005357

[11] Quérel A, Lemaitre P, Brunel M, Porcheron E, Gréhan G (2010) Real-time global interferometric laser imaging for the droplet sizing (ILIDS) algorithm for airborne research, *Measurement Science and Technology*, vol. 21. 015306. doi:10.1088/0957-0233/21/1/015306

[12] Brunel M, Shen H (2013) Design of ILIDS configurations for droplet characterization. *Particuology*, vol. 11, pp 148-157. http://dx.doi.org/10.1016/j.partic.2012.06.014

[13] Shen H, Coëtmellec S, Brunel M (2012) Cylindrical interferometric out-of-focus imaging for the analysis of droplets in a volume, *Optics Letters*, vol. 37, pp 3945–3947. doi: http://dx.doi.org/10.1364/OL.37.003945

[14] Shen H, Coëtmellec S, Brunel M (2013) Simultaneous 3D location and size measurement of spherical bubbles using cylindrical interferometric out-of-focus imaging, *Journal of Quantitative Spectroscopy and Radiative Transfer*, vol. 131, pp 153-159. doi: 10.1016/j.jqsrt.2013.04.009

[15] Brunel M, Shen H, Coëtmellec S, Gréhan G, Delobel T (2014) Determination of the size of irregular particles using interferometric out-of-focus imaging. *International Journal of Optics*, Article ID 143904. doi: http://dx.doi.org/10.1155/2014/143904

[16] Brunel M, Coetmellec S, Gréhan G, Shen H (2014) Interferometric out-of-focus imaging simulator for irregular rough particles. *Journal of the European Optical Society: Rapid Publications*, vol. 9, 14008. doi: http://dx.doi.org/10.2971/jeos.2014.14008

[17] Brunel M, Gonzalez Ruiz S, Jacquot J, van Beeck J (2015) On the morphology of irregular rough particles from the analysis of speckle-like interferometric out-of-focus images. *Optics Communications*, vol. 338, pp 193-198. doi : http://dx.doi.org/10.1016/j.optcom.2014.10.053

[18] Nussenzveig H M (1969) High-frequency scattering by a transparent sphere I: Direct reflection and transmission, *Journal of Mathematical Physics*, vol. 10, pp 82. doi: http://dx.doi.org/10.1063/1.1664764

[19] Glantschnig W J, Chen S H (1981) Light scattering from water droplets in the geometrical optics approximation, *Applied Optics*, vol. 20, pp 2499-2509. doi: http://dx.doi.org/10.1364/AO.20.002499

[20] Van de Hulst H C (1981) Light Scattering by Small Particles, General publishing company.

[21] Shen H, Saengkaew S, Gréhan G, Coëtmellec S, Brunel M (2014) Interferometric out-of-focus imaging for the 3D tracking of spherical bubbles in a cylindrical channel, *Optics Communications*, vol. 320, pp 156-161. doi:10.1016/j.optcom.2014.01.020

[22] Goodman J W (2009) Speckle phenomena in optics. Theory and Applications, Roberts and Company Publishers.